Uluslararası İleri Doğa Bilimleri ve Mühendislik Araştırmaları Dergisi
Sayı 8, S. 545-553, 11, 2024

Araştırma Makalesi

IJANSER
https://as-proceeding.com/index.php/ijanser
ISSN:2980-0811

International Journal of Advanced Natural Sciences and Engineering Researches
Volume 8, pp. 545-553, 11, 2024

Research Article

Optimizing Printing Parameters for Enhanced Mechanical Properties of Carbon Fiber-Reinforced Engineering Filaments in FFF

Güney ULUS[1], Sinan YILMAZ [2*]

[1]*Faculty of Aeronautics and Astronautics, Kocaeli University, Turkey*
[2*] *Department of Mechanical and Material Technologies, Kocaeli University, Turkey*

(sinan.yilmaz@kocaeli.edu.tr)

(Received: 15 December 2024, Accepted: 18 December 2024)

(4th International Conference on Frontiers in Academic Research ICFAR 2024, December 13-14, 2024)

ATIF/REFERENCE: Ulus, G. & Yılmaz, S. (2024). Optimizing Printing Parameters for Enhanced Mechanical Properties of Carbon Fiber-Reinforced Engineering Filaments in FFF. *International Journal of Advanced Natural Sciences and Engineering Researches*, 8(11), 545-553.

Abstract – The demand for improved mechanical performance in 3D printed components has grown with advancements in technology. This study focuses on carbon fiber-reinforced polyethylene terephthalate (PET) and polyamide 12 (PA12) filaments used in the Fused Filament Fabrication (FFF) process. To explore the effects of printing parameters on mechanical properties, the Taguchi experimental design was employed. Four key parameters-layer thickness, infill density, printing temperature, and print speed-were selected at three levels each. Standard tensile specimens were fabricated for each material based on Taguchi's design, and their mechanical properties recorded. Results showed that material properties were sensitive to printing parameters. Statistical analysis revealed that for both materials, layer thickness and infill density were the most influential parameters on mechanical properties, while print speed and temperature had minimal effects. The p-value for the statistical model of tensile strength, tensile modulus, and elongation at break were found below the critical 0.05 threshold for tensile strength and elongation, indicating the model's suitability, except for tensile modulus. Additionally, optimization values for both materials obtained via the statistical model were presented.

Keywords – 3D printing, Fused Filament Fabrication (FFF), Composite Filaments, Mechanical Properties, Experimental Design.

I. INTRODUCTION

Additive manufacturing (AM) methods, which enable the layer-by-layer production of complex parts with minimal material usage and a wide range of design freedom, have become a general term for innovative technologies that have revolutionized the manufacturing industry, requiring little to no post-processing or labor [1]. Under the term additive manufacturing (AM), there are many different methods that enable the layer-by-layer production of metals, ceramics, and polymers, including selective laser sintering (SLS), stereolithography (SLA), direct metal laser sintering (DMLS), electron beam melting (EBM), and fused filament fabrication (FFF) [2]. Among these methods, fused filament fabrication (FFF) stands out for its cost-effectiveness, compact machines, and use of affordable consumables, making it accessible not only to large-scale factories but also to individual users. Its low energy consumption further enhances its appeal, establishing FFF as a versatile and budget-friendly solution in the field of

additive manufacturing. A citizen can even obtain a 3D printer from local chain stores for hobby purposes or educational needs for their children [3,4]. Due to these advantages, the FFF 3D printer market has experienced significant economic growth, driven by its widespread adoption among both industrial and individual users [5]. Some countries have even recognized the potential of economic and technological advancement in the 3D printing sector and have made it a part of their national policies [6].

Fused Filament Fabrication (FFF) is a method where a filament is melted and extruded to form layers on a build plate, with movement in the z-axis after each layer, leading to the creation of a three-dimensional object, which is why it is known as 3D printing. Due to their affordability, accessibility, high specific strengths, wide range of material options, and ability to be shaped through melting, polymers are the most practical materials for the FFF method. The thermoplastics that are best adapted to and widely accepted in the method include polylactic acid (PLA), acrylonitrile butadiene styrene (ABS), polyethylene terephthalate glycol (PETG), polypropylene (PP), and polyamide (PA) [7–9]. However, when used in a neat form, these materials typically exhibit low mechanical properties and are not suitable for manufacturing functional machine parts that are subject to loads or mechanical stresses due to their relatively short operational lifespan. Therefore, they need to be reinforced for use [10]. Particle-reinforced filaments, while providing good results during the printing process, can lead to lower mechanical properties due to challenges such as agglomeration and non-uniform distribution of the reinforcing particles [11]. While continuous fiber reinforcement yields superior mechanical properties, the process challenges limit the use of continuous fiber-reinforced filaments in 3D printing to a narrow range of applications or experimental studies only [12–14]. Therefore, for 3D printing, short fibers are considered the most suitable reinforcement elements, with carbon and glass-based fibers being the most widely used [15].

There is currently no comprehensive research in the literature on CF fiber-reinforced PET and PA12 matrix filaments, as these materials are relatively new to the market, developed to address the growing demands in the 3D printing industry. To fill this gap, this study employed the Taguchi experimental design method to optimize the 3D printing process. The mechanical properties of these materials under tensile stress were systematically assessed by varying key parameters such as layer thickness, infill density, melting temperature, and print speed, allowing for a comparative analysis of their mechanical behaviors.

II. MATERIALS AND METHOD

A. Filaments and Process

Table 1. The characteristics of the filaments as specified in the manufacturer's technical documentation

Material		PA12_CF	PET_CF
Property			
PA12 content (%wt.)		80-88	-
PET content (%wt.)		-	68-89
Pyromellitic dianhydride (%wt.)		-	1-10
Glycerol (%wt.)		-	0-2
Carbon fiber (%wt.)		12-20	10-20
Tensile strength (MPa)		103.2	63.2
Young's modulus (MPa)	XY, ISO527, 5 mm/min, dried	8386	6178
Elongation at break (%)		1.8	3.7
Flexural strength (MPa)		160.7	108
Flexural modulus (MPa)	XY, ISO178, 2 mm/min, dried	8258	5452
Flexural elongation at Break (%)		2.4	3.7
Heat distortion temperature at 0.45 MPa, dried (ºC)		145	108
Glass transition temperature (ºC)		70	79
Crystallization temperature (ºC)		180	204
Melting temperature (ºC)		234	245
Melt volume flow rate (cm^3/10 min)		42.2	25
Filament diameter (mm)		1.75	1.75
Density (g/cm^3)		1.203	1.366
Color		Black	Black
Nozzle temperature (ºC)		260-280	250-270
Print speed (mm/s)		30-80	30-80

The test specimens were produced using a Creality CR-M4 3D (FFF) printer in combination with two different Ultrafuse® composite filaments. The G-code files required for printing were prepared using Creality Print software (Version 4.3.7.6619). During the generation of G-codes, all factors not selected for the experimental design (e.g., initial layer thickness, number of walls, bed temperature, etc.) were maintained at the software's default values for the PA material. Prior to printing, filament materials were dried in a vacuum oven at 65°C for 12 hours to remove any residual moisture. The properties of the filament materials and the 3D printing parameters, as recommended by the manufacturer, are detailed in Table 1.

B. Design of Experiments

Variables that affect the outcome of a process are called parameters. For FFF 3D printing, there are many parameters, but the most influential ones are layer thickness, print speed, infill density, and print temperature. Therefore, an experimental design, as presented in Table 2, was created using the Taguchi method for these parameters. The selection of the values in Table 2 was based on the recommendations of the manufacturer (see Table 1).

Table 2. Optimization of Printing Parameters

Factor	Level	Value
Layer Thickness (mm)	3	0.1, 0.2, 0.3
Infill Density (%)	3	25, 50, 100
Print Speed (mm/s)	3	60, 70, 80
Print Temperature (ºC)	3	260, 265, 270

According to the design presented in Table 2, Table 3 was prepared using Minitab V. 20.4 software. This experimental design allowed for a reduction in the number of tests conducted. By applying the Taguchi method, a total of 9 test sets for each material were conducted, significantly reducing the number

of experiments compared to the 81 combinations of parameters that would have been required without this approach.

Table 3. Design of Experiment (DOE) Matrix

Sample (Code)	Layer Thickness (mm)	Infill Density (%)	Print Temperature (°C)	Print Speed (mm/s)
IT1	0.1	25	260	60
IT2	0.1	50	265	70
IT3	0.1	100	270	80
IT4	0.2	25	265	80
IT5	0.2	50	270	60
IT6	0.2	100	260	70
IT7	0.3	25	270	70
IT8	0.3	50	260	80
IT9	0.3	100	265	60

C. Tensile Tests

The tensile tests were performed on 3D printed ISO Type 5A specimens at ambient temperature using an Instron 4411 universal testing machine. The tests were conducted at a consistent strain rate of 5 mm/min. Mechanical properties such as tensile strength at yield (σ_y), tensile modulus (E), and elongation at break (ε) were measured, with data collected from at least three individual samples to determine the mean and standard deviation values.

D. Response Surface Method (RSM)

RSM is a statistical technique used to explore the relationship between input variables and response, optimizing process parameters while minimizing the number of experiments. It involves fitting a polynomial regression model to experimental data to efficiently analyze and improve a process [16].This method was applied in combination with the Taguchi experimental design approach to identify the most influential parameters and optimize the 3D printing process. The analysis was conducted using Minitab V. 20.4 software to ensure a comprehensive and accurate evaluation of the data.

III. RESULTS AND DISCUSSION

The findings of the tests conducted according to the DOE are presented graphically in Figure 1 and listed in Table 4. Examining the graph in Fig 1 for σ_y and E reveals that the highest values for both materials can be achieved with the IT3 combination. On the other hand, for ε, no clear conclusion can be drawn for either material when considering the standard deviation values. Examining Fig. 1a closely reveals that, while the trends are similar, the yield strength of PA12_CF is more noticeably affected by varying process conditions compared to PET_CF. Similarly, a comparable observation can be made for the modulus graph in Fig. 1b. In Fig. 1c, PA12_CF and PET_CF exhibit different trends. This divergence is attributed to the higher error bars and lower average values for PET_CF.

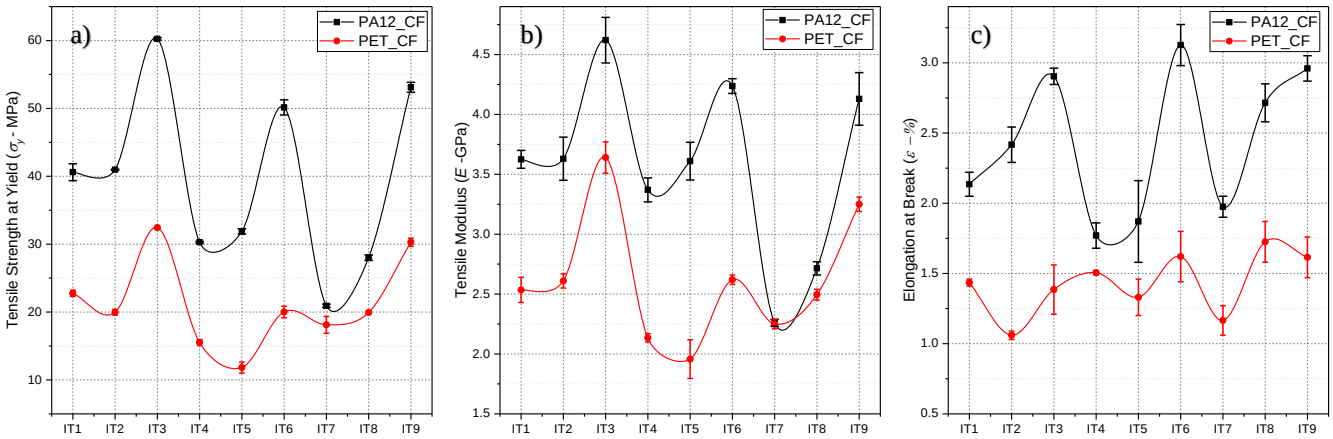

Fig. 1. Uniaxial tensile test results: a) yield strength, b) modulus, c) elongation at break

Table 4. Tensile test results of the materials for DOE codes

MATERIAL	*PA12_CF*			*PET_CF*		
CODE	σ_y (MPa)	*E* (GPa)	*ε (%)*	σ_y (MPa)	*E* (GPa)	*ε (%)*
IT1	40.6 ±1.2	3.6 ±0.1	2.1 ±0.1	22.8 ±0.5	2.5 ±0.1	1.4 ±0.0
IT2	41.0 ±0.1	3.6 ±0.2	2.4 ±0.1	20.0 ±0.4	2.6 ±0.1	1.1 ±0.0
IT3	60.3 ±0.2	4.6 ±0.2	2.9 ±0.1	32.4 ±0.1	3.6 ±0.1	1.4 ±0.2
IT4	30.3 ±0.1	3.4 ±0.1	1.8 ±0.1	15.5 ±0.4	2.1 ±0.0	1.5 ±0.0
IT5	31.9 ±0.4	3.6 ±0.2	1.9 ±0.3	11.8 ±0.8	2.0 ±0.2	1.3 ±0.1
IT6	50.2 ±1.1	4.2 ±0.1	3.1 ±0.1	20.0 ±0.8	2.6 ±0.0	1.6 ±0.2
IT7	20.9 ±0.2	2.3 ±0.0	2.0 ±0.1	18.1 ±1.2	2.3 ±0.0	1.2 ±0.1
IT8	28.0 ±0.4	2.7 ±0.1	2.7 ±0.1	19.9 ±0.2	2.5 ±0.0	1.7 ±0.1
IT9	53.1 ±0.7	4.1 ±0.2	3.0 ±0.1	30.3 ±0.6	3.3 ±0.1	1.6 ±0.1

The tensile yield strength values obtained in this study, averaged for the 100% infill specimens (IT3, IT6, IT9) listed in Table 4, were 54.5 MPa for PA12_CF and 27.6 MPa for PET_CF, which are 47.2% and 56.3% lower than the manufacturer's reported values provided in Table 1, respectively. The Young's modulus values for 100% infill specimens were 4.3 GPa for PA12_CF and 3.2 GPa for PET_CF, which are 48.7% and 48.7% lower than the manufacturer's reported values, respectively. The elongation at break values for PA12_CF and PET_CF were 4.3% and 3.2%, respectively. These values are 2.5% higher for PA12_CF and 0.5% lower for PET_CF compared to the manufacturer's reported values. Unlike the manufacturer's datasheet, which indicates that PA12_CF has lower elongation at break than PET_CF, the results of this study show that PA12_CF exhibits more ductile fracture behavior.

The Analysis of Variance (ANOVA) of the measured tensile properties is presented in Tables 5, 6 and 7 for σ_y, E and ε respectively. Examining the ANOVA results for the mechanical test data, as shown in Table 5, reveals that the *p*-value, which measures the statistical model's accuracy, is calculated as 0.002 for yield strength. For modulus, this value is 0.075, and for elongation at break, it is 0.025.

The Pareto chart obtained from the ANOVA analysis to examine the effect of the selected four 3D print parameters on yield stress is presented in Fig. 2. The graph clearly shows that the most influential parameter is the infill density, followed by the layer thickness. It can be said that the 3D printing temperature and printing speed have almost no effect on the results. This is because the selected values are very close to each other. Specifically, the experimental design was created with a difference of 5 degrees in temperature and 10 mm/s in speed. The reason for keeping the ranges so close is to enable a comparison between the two materials.

Table 5. ANOVA of σ_y

Source	DF	Adj SS	Adj MS	F-Value	P-Value
Model	13	3188.72	245.29	35.33	0.002
Linear	5	2618.74	523.75	75.43	0.000
Layer Thickness (mm)	1	181.12	181.12	26.09	0.007
Infill Density (%)	1	800.96	800.96	115.36	0.000
Print Temperature (°C)	1	3.05	3.05	0.44	0.544
Print Speed (mm/s)	1	1.36	1.36	0.20	0.681
Material	1	1632.25	1632.25	235.08	0.000
Square	4	266.70	66.67	9.60	0.025
Layer Thickness (mm)*Layer Thickness (mm)	1	128.44	128.44	18.50	0.013
Infill Density (%)*Infill Density (%)	1	85.95	85.95	12.38	0.024
Print Temperature (°C)*Print Temperature (°C)	1	15.16	15.16	2.18	0.214
Print Speed (mm/s)*Print Speed (mm/s)	1	37.14	37.14	5.35	0.082
2-Way Interaction	4	281.44	70.36	10.13	0.023
Layer Thickness (mm)*material	1	90.48	90.48	13.03	0.023
Infill Density (%)*material	1	180.13	180.13	25.94	0.007
Print Temperature (°C)*material	1	2.42	2.42	0.35	0.587
Print Speed (mm/s)*material	1	8.41	8.41	1.21	0.333
Error	4	27.77	6.94		
Total	17	3216.49			

Table 6. ANOVA of E

Source	DF	Adj SS	Adj MS	F-Value	P-Value
Model	13	10.1608	0.78160	4.63	0.075
Linear	5	8.7015	1.74030	10.30	0.021
Layer Thickness (mm)	1	1.0561	1.05613	6.25	0.067
Infill Density (%)	1	3.3303	3.33029	19.71	0.011
Print Temperature (°C)	1	0.0010	0.00101	0.01	0.942
Print Speed (mm/s)	1	0.0014	0.00144	0.01	0.931
Material	1	4.3126	4.31260	25.52	0.007
Square	4	0.5798	0.14495	0.86	0.557
Layer Thickness (mm)*Layer Thickness (mm)	1	0.1006	0.10063	0.60	0.483
Infill Density (%)*Infill Density (%)	1	0.1716	0.17160	1.02	0.371
Print Temperature (°C)*Print Temperature (°C)	1	0.0790	0.07902	0.47	0.532
Print Speed (mm/s)*Print Speed (mm/s)	1	0.2285	0.22854	1.35	0.310
2-Way Interaction	4	0.5563	0.13908	0.82	0.573
Layer Thickness (mm)*material	1	0.3267	0.32670	1.93	0.237
Infill Density (%)*material	1	0.1052	0.10525	0.62	0.474
Print Temperature (°C)*material	1	0.0067	0.00669	0.04	0.852
Print Speed (mm/s)*material	1	0.1177	0.11768	0.70	0.451
Error	4	0.6759	0.16898		
Total	17	10.8368			

Table 7. ANOVA of ε

Source	DF	Adj SS	Adj MS	F-Value	P-Value
Model	13	6.78979	0.52229	8.74	0.025
Linear	5	6.44443	1.28889	21.58	0.005
Layer Thickness (mm)	1	0.05603	0.05603	0.94	0.388
Infill Density (%)	1	1.09505	1.09505	18.33	0.013
Print Temperature (°C)	1	0.37749	0.37749	6.32	0.066
Print Speed (mm/s)	1	0.03612	0.03612	0.60	0.480
Material	1	4.87974	4.87974	81.69	0.001
Square	4	0.05667	0.01417	0.24	0.904
Layer Thickness (mm)*Layer Thickness (mm)	1	0.03043	0.03043	0.51	0.515
Infill Density (%)*Infill Density (%)	1	0.00063	0.00063	0.01	0.923
Print Temperature (°C)*Print Temperature (°C)	1	0.01487	0.01487	0.25	0.644
Print Speed (mm/s)*Print Speed (mm/s)	1	0.01073	0.01073	0.18	0.693
2-Way Interaction	4	0.58583	0.14646	2.45	0.203
Layer Thickness (mm)*material	1	0.01541	0.01541	0.26	0.638
Infill Density (%)*material	1	0.55849	0.55849	9.35	0.038
Print Temperature (°C)*material	1	0.00898	0.00898	0.15	0.718
Print Speed (mm/s)*material	1	0.00296	0.00296	0.05	0.835
Error	4	0.23893	0.05973		
Total	17	7.02872			

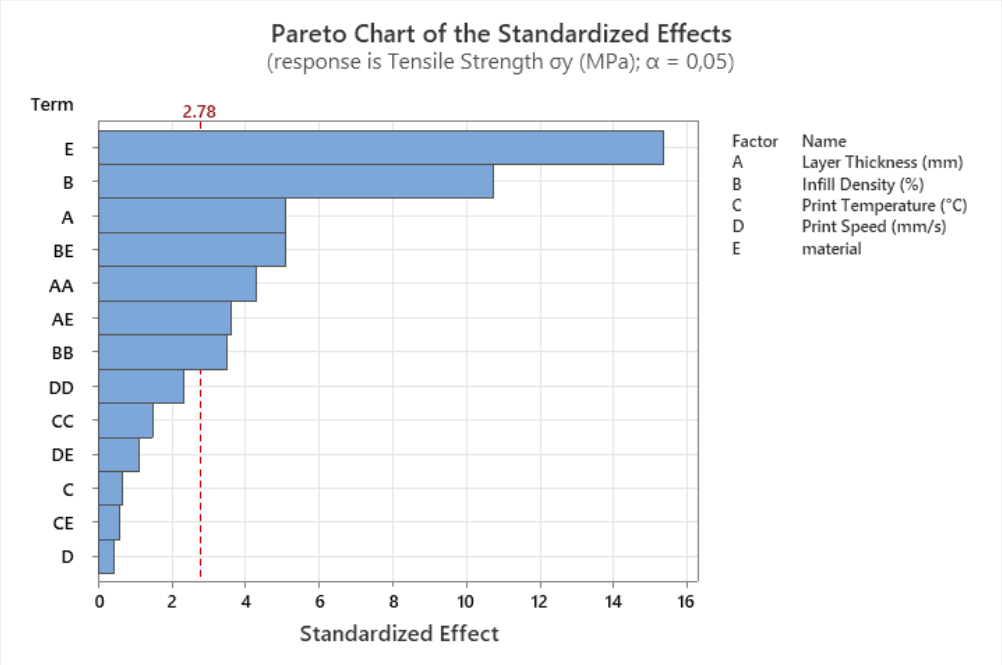

Fig. 2. Pareto chart demonstrating the effect of print parameters on yield stress.

Optimized values of process parameters for maximum mechanical properties were calculated via RSM and listed in Table 8. Examining the table, it is observed that the optimal layer thickness for both materials is 0.1 mm. On the other hand, for the three characteristic mechanical properties, PA12_CF exhibits superior material properties compared to PET_CF.

Table 8. Response optimization solution for both materials

Solution	Material	Layer Thickness (mm)	Infill Density (%)	Print Temperature (°C)	Print Speed (mm/s)	σ_y (MPa) Fit	E (GPa) Fit	ε (%) Fit
1	PET_CF	0.1	100	260	80	31.5	3.4	1.6
2	PA12_CF	0.1	100	260	80	63.1	4.7	3.3

IV. CONCLUSION

This study systematically evaluated the mechanical properties of carbon fiber-reinforced PET (PET_CF) and PA12 (PA12_CF) filaments used in the Fused Filament Fabrication (FFF) process. The results from the tensile tests, conducted under varying printing parameters, provide significant insights into how these factors influence material properties. Layer thickness and infill density were identified as the most influential parameters on the mechanical properties of both materials, while print temperature and print speed had minimal effects, likely due to the narrow variation ranges applied during testing. PA12_CF demonstrated superior mechanical performance compared to PET_CF, with a maximum tensile yield strength of 60.3 MPa, which is approximately 86% higher than PET_CF's 32.4 MPa. Additionally, PA12_CF exhibited a higher modulus by 28%, and a greater elongation at break of 4.3%, which was 2.5% higher than the manufacturer's reported value, indicating more ductile fracture behavior. The statistical analysis revealed a significant correlation between the printing parameters and tensile yield strength, with a p-value of 0.002. The optimal printing conditions for achieving the highest tensile properties for both materials were found to be a 0.1 mm layer thickness, 100% infill density, 270°C print temperature, and 80 mm/s print speed. These findings emphasize the importance of carefully selected printing parameters to maximize the mechanical performance of carbon fiber-reinforced filaments in FFF applications.

REFERENCES

[1] Yilmaz S, Gul O, Eyri B, Gamze Karsli Yilmaz N, Yilmaz T. Comprehensive characterization of 3D-printed bamboo/poly(lactic acid) bio composites. Polym Eng Sci 2023;63:2958–72. https://doi.org/10.1002/pen.26419.

[2] Yilmaz S, Eyri B, Gul O, Karsli NG, Yilmaz T. Investigation of the influence of salt remelting process on the mechanical, tribological, and thermal properties of 3D-printed poly(lactic acid) materials. Polym Eng Sci 2024;64:17–30. https://doi.org/10.1002/pen.26526.

[3] Podgórski R, Wojasi´nski MW, Ciach T. HardwareX 16 (2023) e00486 Pushing boundaries in 3D printing: Economic pressure filament extruder for producing polymeric and polymer-ceramic filaments for 3D printers 2023. https://doi.org/10.17605/OSF.IO/X3FZN.

[4] Alami AH, Mahmoud M, Aljaghoub H, Mdallal A, Abdelkareem MA, Kamarudin SK, et al. Progress in 3D printing in wind energy and its role in achieving sustainability. International Journal of Thermofluids 2023;20. https://doi.org/10.1016/j.ijft.2023.100496.

[5] Yilmaz S. Comparative Investigation of Mechanical, Tribological and Thermo-Mechanical Properties of Commonly Used 3D Printing Materials. European Journal of Science and Technology 2022. https://doi.org/10.31590/ejosat.1040085.

[6] Liu Q. Evaluating the Impact of 3D Printing Technology Innovations on Industrial Production Efficiency and Economic Growth in the Automotive Sector in China. Innovation in Science and Technology 2024;3:60–6. https://doi.org/10.56397/ist.2024.05.07.

[7] Wong K V., Hernandez A. A Review of Additive Manufacturing. ISRN Mechanical Engineering 2012;2012:1–10. https://doi.org/10.5402/2012/208760.

[8] Kumar S, Singh R, Singh TP, Batish A. Fused filament fabrication: A comprehensive review. Journal of Thermoplastic Composite Materials 2020:1–21. https://doi.org/10.1177/0892705720970629.

[9] Odera RS, Idumah CI. Novel advancements in additive manufacturing of PLA: A review. Polym Eng Sci 2023:1–20. https://doi.org/10.1002/pen.26450.

[10] Wang X, Jiang M, Zhou Z, Gou J, Hui D. 3D printing of polymer matrix composites: A review and prospective. Compos B Eng 2017;110:442–58. https://doi.org/10.1016/j.compositesb.2016.11.034.

[11] Yilmaz S, Gul O, Eyri B, Karsli NG, Yilmaz T. Analyzing the Influence of Multimaterial 3D Printing and Postprocessing on Mechanical and Tribological Characteristics. Macromol Mater Eng 2024;309. https://doi.org/10.1002/mame.202300428.

[12] Todoroki A, Oasada T, Mizutani Y, Suzuki Y, Ueda M, Matsuzaki R, et al. Tensile property evaluations of 3D printed continuous carbon fiber reinforced thermoplastic composites. Advanced Composite Materials 2020;29:147–62. https://doi.org/10.1080/09243046.2019.1650323.

[13] Mohammadizadeh M, Fidan I. Tensile performance of 3d-printed continuous fiber-reinforced nylon composites. Journal of Manufacturing and Materials Processing 2021;5. https://doi.org/10.3390/jmmp5030068.

[14] Tian X, Todoroki A, Liu T, Wu L, Hou Z, Ueda M, et al. 3D Printing of Continuous Fiber Reinforced Polymer Composites: Development, Application, and Prospective. Chinese Journal of Mechanical Engineering: Additive Manufacturing Frontiers 2022;1:100016. https://doi.org/10.1016/j.cjmeam.2022.100016.

[15] Yilmaz S. Comprehensive analysis of 3D printed PA6.6 and fiber-reinforced variants: Revealing mechanical properties and adhesive wear behavior. Polym Compos 2023;45:1446–60. https://doi.org/10.1002/pc.27865.

[16] Yarar E, Sinmazçelik T. Effect of solid lubricant reinforcing on drilling performance of castamide and thermal analysis. Journal of Vinyl and Additive Technology 2024. https://doi.org/10.1002/vnl.22124.